POPULATION STUDIES OF *INTEGRAL* SOURCES

A. Bodaghee[1], T.J.-L. Courvoisier[1], J. Rodriguez[2], V. Beckmann[3], N. Produit[4], D. Hannikainen[5], and E. Kuulkers[6]

[1]INTEGRAL *Science Data Centre, Chemin d'Ecogia 16, CH–1290 Versoix, Switzerland, arash.bodaghee@obs.unige.ch*
[1]*Observatoire Astronomique de l'Université de Genève, Chemin des Maillettes 51, CH–1290 Sauverny, Switzerland*
[2]*CEA-Saclay/DSM/DAPNIA/SAp, 91191 Gif-sur-Yvette, France, jrodriguez@cea.fr*
[3]*NASA Goddard Space Flight Center, Astrophysics Science Division, Greenbelt, MD 20771, USA, beckmann@milkyway.gsfc.nasa.gov*
[4]INTEGRAL *Science Data Centre, Chemin d'Ecogia 16, CH–1290 Versoix, Switzerland, nicolas.produit@obs.unige.ch*
[4]*Observatoire Astronomique de l'Université de Genève, Chemin des Maillettes 51, CH–1290 Sauverny, Switzerland*
[5]*Observatory, P.O. Box 14, FI-00014 University of Helsinki, Finland, diana@astro.helsinki.fi*
[6]*ISOC, ESA/ESAC, Urb. Villafranca del Castillo, P.O. Box 50727, 28080 Madrid, Spain, erik.kuulkers@sciops.esa.int*

ABSTRACT

INTEGRAL-ISGRI has detected over 300 sources in its first 3 years of observations. We have collected the parameters of these sources from the literature ($N_{\rm H}$, spin and orbital periods, and distances or redshifts) in order to test correlations expected from theoretical predictions, and to investigate where the new and previously-known sources detected by ISGRI fit in the parameter space of high-energy objects. The influence of the local absorbing matter on the modulations is studied for High-Mass X-ray Binaries with OB supergiant and Be companions. In this context, we find that High-Mass X-ray Binaries are generally segregated in plots of intrinsic $N_{\rm H}$ versus the orbital period of the system and versus the spin period of the pulsar, based on whether the companion is a Be or OB supergiant star. We also find a tentative but expected anti-correlation between $N_{\rm H}$ and the orbital period, and a possible and unexpected correlation between the $N_{\rm H}$ and the spin period.

Key words: Gamma-rays: surveys, catalogs – X-rays: binaries.

1. INTRODUCTION

In just over 3 years, *INTEGRAL*-IBIS [1, 2] has detected $\sim$ 350 sources in the hard X to soft γ-ray band (20–100 keV), among which $\sim$ 140 sources were previously unknown at hard X-ray energies. We will hereafter refer to the latter sources as IGRs [1] (*INTEGRAL* Gamma-Ray sources). Most of the sources that IBIS/ISGRI has detected are Galactic Low and High-Mass X-ray Binaries (LMXBs and HMXBs, respectively) or Active Galactic Nuclei (AGN). Both LMXBs and HMXBs feature a compact object such as a neutron star (NS) or a black hole (BH) accreting material from a companion star: a faint old dwarf in LMXBs (M $\lesssim$ 1 M$_\odot$), a bright young giant in HMXBs (M $\gtrsim$ 10 M$_\odot$), or sometimes an intermediate-mass companion. Accretion typically occurs via Roche-lobe overflow in LMXBs or through the wind in HMXBs. An accretion disk can be found in both types of systems and is an important component of the optical/UV and X-ray emission from AGN and LMXBs.

Subclasses exist within the 3 most common groups. In the case of HMXBs, the spectral type of the stellar companion determines the sub-classification beyond the NS or BH nature of the compact object. A majority of HMXBs host main-sequence (MS) Be stars that have not filled their Roche lobe [3]. These systems are usually transient with flares produced whenever the sometimes wide and eccentric orbit brings the compact object close to its companion. Persistent HMXBs are typically accompanied by an evolved supergiant (SG) O or B star whose wind steadily feeds the compact object. Their variability stems from inhomegeneities in the wind. Similarly, LMXBs can be classified based on the type of compact object (NS or BH) it has. Neutron star LMXBs can be divided further into Z or Atoll sources depending on the tracks they follow in a color-color diagram. The 2 primary groups of AGN are Seyfert 1 and 2, with the latter being more absorbed and showing narrow emission lines only.

Our understanding of the different populations of *INTEGRAL* sources is limited by the large number of sources about which very little is known. Roughly half of all IGRs remain unclassified. The nature of these sources is difficult to elucidate given that many are faint or transient. Furthermore, the imaging, spectral, and timing analyses gathered from a single energy range are usually insufficient to classify an object. Information from other wavelengths such as soft X-rays, infrared or radio are necessary to help identify a source. For example, ra-

[1] an updated list of IGRs can be found at http://isdc.unige.ch/~rodrigue/html/igrsources.html

*Table 1. The number of sources from each of the major classes detected by ISGRI are listed for new (≡ IGRs) or previously known (≡ pre-*INTEGRAL*) sources. Miscellaneous refers to sources such as CVs, SNRs, AXPs, etc., while Uncl. denotes sources whose classification is unknown. Also provided are the percentages of the different source types as a fraction of the total. For sources whose classifications are known, the second percentage gives the proportion that such sources represent with respect to the classified sources.*

	HMXBs	LMXBs	AGN	Misc.	Uncl.	Total
IGRs	30 (21%, 35%)	3 (2%, 3%)	39 (28%, 45%)	14 (10%, 16%)	56 (39%)	142
pre-*INTEGRAL*	40 (20%, 21%)	73 (36%, 39%)	49 (24%, 26%)	25 (13%, 13%)	14 (7%)	201
Total *INTEGRAL*	70 (20%, 26%)	76 (22%, 28%)	88 (26%, 32%)	39 (11%, 14%)	70 (20%)	343

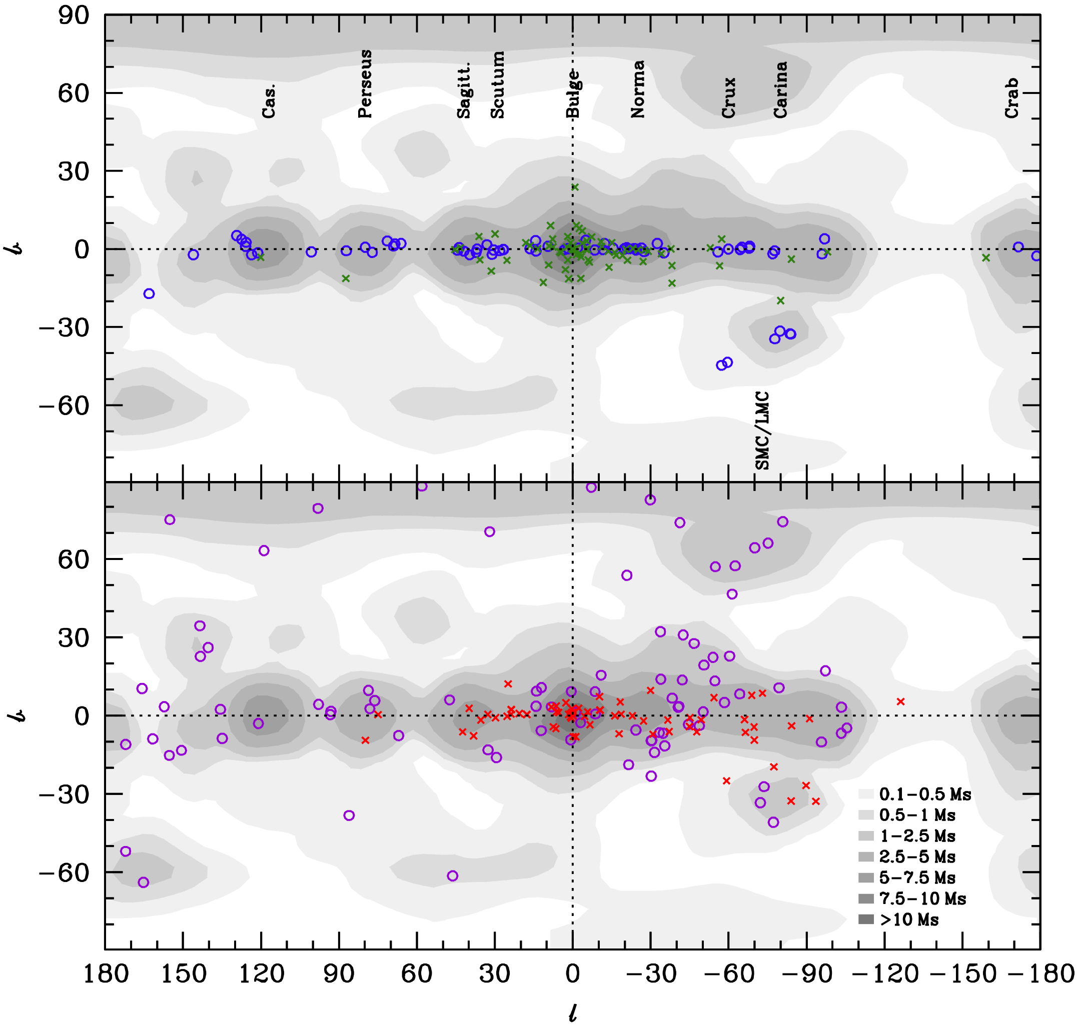

Figure 1. Spatial distribution in Galactic coordinates of sources detected so far by ISGRI. The figure at the top presents the distributions of LMXBs (crosses) and HMXBs (circles), while the figure at the bottom shows unclassified sources (crosses) and extragalactic sources (circles). Miscellaneous sources have been omitted for clarity. The directions to the spiral arm tangents and other areas of interest are indicated, as are the cumulative exposure times at each location (from public data in revs. 30–405). The number of sources in each class are listed in Table 1.

dio emission can be the signature of a jet or pulsar, while the optical spectral type can help distinguish between LMXBs and HMXBs, and the redshift can place it at extragalactic distances. Follow-up observations with soft X-ray telescopes (i.e. *Chandra*, *RXTE*, *Suzaku*, *Swift* and *XMM-Newton*) can provide fine timing analyses which enable short-period modulations to be found, and they can describe the shape of the continuum below ISGRI's ~20 keV lower limit, in an energy range where potential photoelectric absorption (N_{H}) and iron fluorescence lines

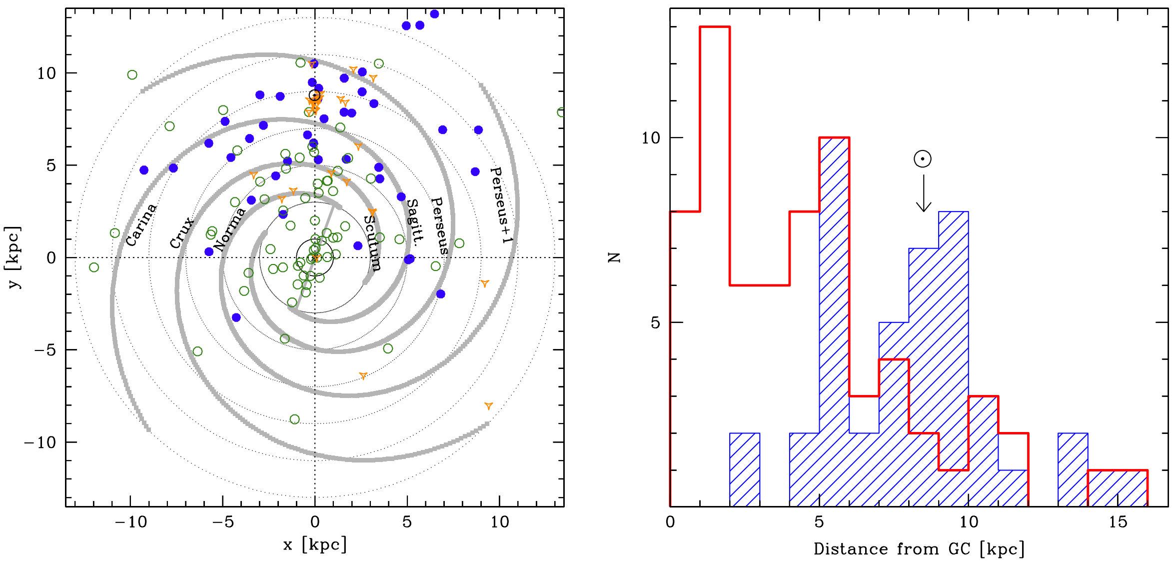

Figure 2. left: *Galactic distribution of HMXBs (44, filled circles), LMXBs (68, empty circles), and miscellaneous sources (33, triangles). Also plotted is a modified spiral arm model [14] with the Sun at 8.5 kpc from the center and a pitch angle of 14°.* right: *Distribution of galactocentric distances of HMXBs (shaded histogram) and LMXBs (clear histogram).*

are detectable. Precise X-ray coordinates from *Chandra*, *Swift* or *XMM-Newton* can be used to search for counterparts in dedicated radio, optical, and IR observations or in catalogs. However, many sources are clustered in the Galactic center and along the plane, which, because of the density of stars and the amount of obscuring dust, can hinder the identification of the optical/IR counterpart.

Perhaps the most interesting result from follow-up observations is that a number of IGRs present column densities that are much higher than would be expected along the line of sight. These large absorptions are therefore intrinsic and could be the reason these sources eluded discovery with previous (softer) X-ray missions. The first new source discovered by *INTEGRAL* is IGR J16318−4848 [4] which is the most absorbed Galactic source known with $N_{\mathrm{H}} \sim 2 \cdot 10^{24}$ atoms·cm^{-2} or roughly 2 orders of magnitude more than the intervening Galactic material [5]. Since this discovery, other sources joined the growing class of heavily-obscured X-ray sources described by [6] and [7]. A certain number of these absorbed sources consist of X-ray pulsars: e.g. IGR J16320−4751 [8], IGR J16393−4643 [9], and IGR J17252−3616 [10].

This research presents the parameters of all sources detected by ISGRI during the first 3 years of *INTEGRAL* observations. Absorption values, pulse and orbital periods, and distances or redshifts were collected from the literature and were used to test various correlations expected from theoretical predictions, and to investigate where the new and old sources detected by ISGRI fit in the parameter space of high-energy objects.

2. DATA & ANALYSIS

We selected all sources from the upcoming Version 27 of the *INTEGRAL* General Reference Catalog [12] which were detected by ISGRI according to Astronomer's Telegrams, IAUCs or in an article. This does not consider the significance or exposure time used to make the declaration. An exposure map was created that accumulated all public pointings in revolutions 30–405 (UTC: 11/1/2003–8/2/2006). After 3 years of observations, the exposure map still favors the Galactic plane and center. Therefore, the completeness of the sample is debatable since this catalog groups all sources that were active above 20 keV while within the ISGRI FOV at some point during the last 3 years.

A number of IGRs have soft X-ray counterparts that were sometimes detected by earlier missions. For example, IGR J16393−4643 was known as AX J1639.0−4642 by *ASCA*, while IGR J17252−3616 was designated EXO 1722−360 by *EXOSAT*, and many IGRs have ROSAT counterparts [13]. Since ISGRI was the first to detect them above 20 keV, it is legitimate to group them together as a population of new soft γ-ray sources. They can then be compared to sources detected by ISGRI that were previously-known to emit above 20 keV (e.g., Crab, Vela X-1, etc.).

The name or position of each source was queried to the SIMBAD and ADS servers for references that could provide any of the following parameters: position and error radius, classification, column density (N_{H}), spin period, orbital period, and distance (or redshift). These values and their references will be presented in an online form of an upcoming article. The positions are from

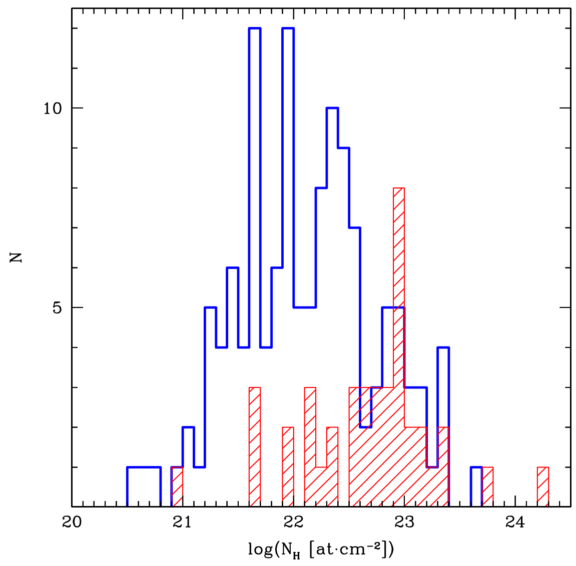

Figure 3. The distribution of reported column densities (N_H) for Galactic sources (including sources in the Magellanic Clouds) detected by ISGRI that were previously known (132, clear histogram) and for IGRs (41, shaded histogram).

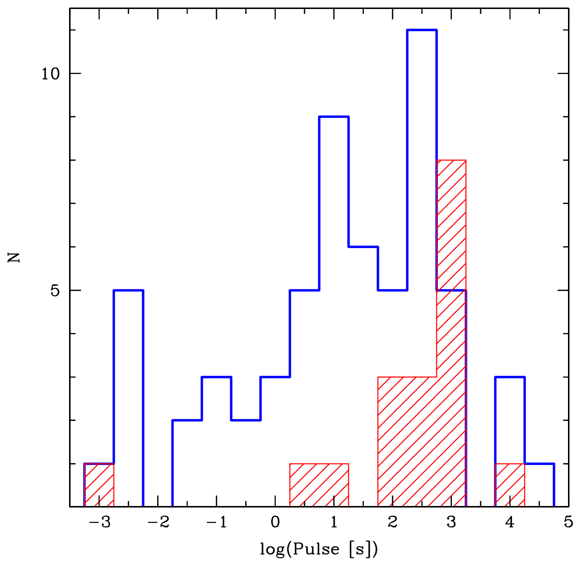

Figure 4. Spin periods reported for X-ray binaries detected by ISGRI that were previously known (61, clear histogram) and for IGRs (18, shaded histogram).

the X-rays unless a more refined position at other wavelengths is known for a confirmed counterpart. Besides a rough X-ray position, very little is known about some sources, while other sources were so thoroughly studied that choices had to be made between sometimes conflicting values (notably N_H and distance). In every case, we favored the most precise or most recent values.

Column densities were gathered from the literature whenever a model fit to the X-ray spectrum required an absorption component. Extracting a single N_H for a source and comparing this value to those of other sources is not a straightforward exercise since intrinsic column densities are not static. A measurement made during flaring or quiescent periods, or at different orbital epochs, will heavily influence the N_H. The geometry of the system, the energy range of the satellite that gathered the data, and the model used to describe the resulting spectrum also affect the N_H value. Therefore, the uncertainties are often large or only upper limits are provided. Whenever possible, we selected the N_H value of the model that best fits a recent X-ray spectrum taken with a telescope that covers the soft X-ray domain well.

Opposing opinions about the distances to Galactic sources make it difficult to settle on a single value or even range. In most cases, the methods used to determine the distance rely on conversions of either X-ray luminosity or stellar effective temperature so the distance uncertainties quoted in the literature can be quite large.

3. RESULTS

3.1. Spatial Distribution

Table 1 lists the major source populations detected by ISGRI that are either new (≡ IGRs) or previously known (≡ pre-*INTEGRAL* sources). ISGRI has discovered many new HMXBs and AGN. Their proportions with respect to other sources are similar to what was known before the launch of *INTEGRAL*. There are few new LMXBs discovered by ISGRI because LMXBs are generally less obscured than HMXBs and so have already been detected by previous satellites. Over 50 new sources await classification. ISGRI has also detected other types of Galactic objects such as Cataclysmic Variables (CVs), Supernova Remnants (SNRs), Anomolous X-ray Pulsars (AXPs), etc., which are referred to henceforth as Miscellaneous.

Naturally, ISGRI detects sources in regions that are exposed (Fig. 1). Given the heterogeneous exposure map of the sky gathered in the last 3 years of observations, detections are biased towards regions of the sky that have been exposed the longest (i.e. the Galactic plane and bulge). However, the evolution of each type of source also plays a role in its spatial distribution. Typical of an old stellar population, LMXBs are concentrated in the Galactic bulge and have had time to migrate to high latitudes. On the other hand, HMXBs are young systems so they must remain close to regions of recent stellar formation. Thus, HMXBs are confined to the Galactic plane with peaks toward the spiral arms.

The distribution of unclassified sources more closely resembles a Galactic distribution rather than an extragalac-

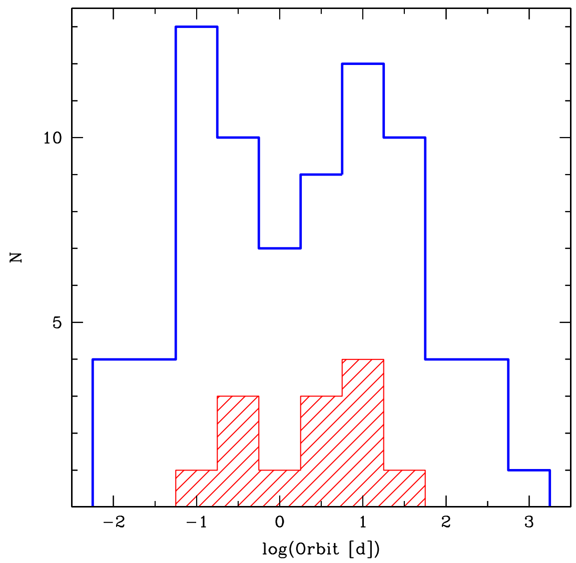

Figure 5. Published orbital periods of X-ray binaries detected by ISGRI. The clear histogram represents sources that were previously known (78) while the shaded histogram represents IGRs (13).

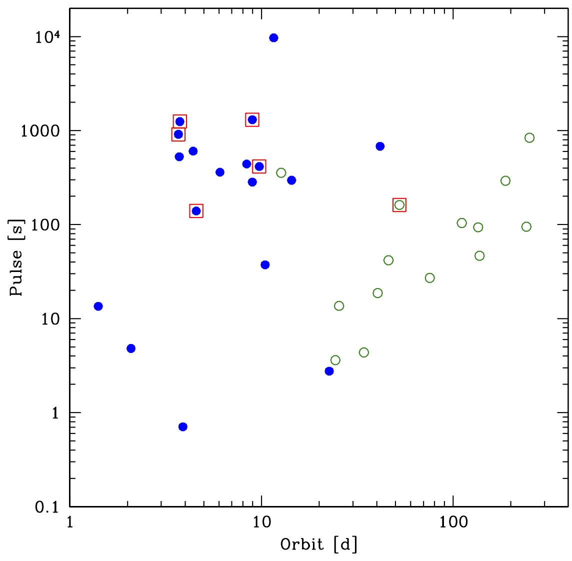

Figure 6. Corbet diagram of spin vs. orbital period of HMXBs detected by ISGRI whose companions are OB supergiants (18, filled circles) or Be stars (14, empty circles). IGRs are boxed.

tic one (Fig. 1, bottom). Many of the unclassified sources could be AGN situated behind the Galactic plane [15], but their distribution suggests that these sources are probably X-ray binaries from the Milky Way and Magellanic Clouds, and nearby Galactic sources such as CVs.

Another way to demonstrate the role of stellar evolution in shaping the spatial distributions of LMXBs and HMXBs is to plot the positions of sources whose distances are known on a spiral-arm model of the galaxy [14]. This model has been slightly modified to place the Sun at 8.5 kpc from the Galactic Center (GC) and each arm has a pitch angle of 14°. While the uncertainties on distances can be large, Fig. 2 shows that HMXBs tend to occupy the outer disk and arms where young stars are formed, whereas LMXBs are clustered near the bulge where old globular clusters reside. A histogram of galactocentric radii (Fig. 2, right) shows LMXBs peaked at the center and decreasing gradually, while HMXBs follow the distributions from HII/CO surveys which are under-abundant in the central few kpc and peak at the spiral arms. It is interesting to note that [16] and [17] suggest an offset in the distribution of HMXBs with respect to the directions of the spiral arm tangents. This implies a delay between the epoch of star formation and the time when the number of HMXBs reaches its maximum. We will investigate this problem in a future paper.

Fig. 2 appears to show an asymmetry of LMXBs in the central 3 kpc of the galaxy. Within 3 kpc of the center, ISGRI has detected more LMXBs (whose distances are known) with negative longitudes as those with positive longitudes (a ratio of 16:11), and only 1 LMXB has been detected in the Galactic center region bound by $0 < x < 3$ kpc and $-3 < y < 0$ kpc (see Fig. 2, left). While no asymmetry is expected from maps of Galactic absorption [5], the bar could be responsible for preventing an identification and distance measurement to be made for counterparts to LMXBs situated behind it. The left-right asymmetry is reduced by assigning a distance of 8.5 kpc to LMXBs in this direction whose distances are unknown (a ratio of 34:29).

3.2. Absorption

Column densities of some sources in our sample are higher than the expected value along the line of sight as obtained by [5] which implies absorbing material intrinsic to the source. If accreted, this material will add to the emission regardless of its orientation with respect to the compact object and the observer's line of sight, while also obscuring it whenever it eclipses the X-ray source.

On average, Galactic IGRs are more absorbed than the sources seen before *INTEGRAL* (by a factor of ~4) with IGRs representing a sizable contingent of objects that have $N_H \sim 10^{23}$ atoms·cm^{-2} (see Fig. 3). The average column density of sources that were previously known is $N_H = 1.2 \cdot 10^{22}$ atoms·cm^{-2} ($\sigma \sim 0.7$) whereas IGRs have an average $N_H = 4.8 \cdot 10^{22}$ atoms·cm^{-2} ($\sigma \sim 0.6$). A Kolmogorov-Smirnov (KS) test yields a probability of less than 0.01% that the two distributions are statistically compatible.

The classified Galactic IGRs are mostly HMXBs (Table 1) which usually exhibit high column densities, either intrinsically due to the geometry of the system or extrinsically due to their location along the dusty Galac-

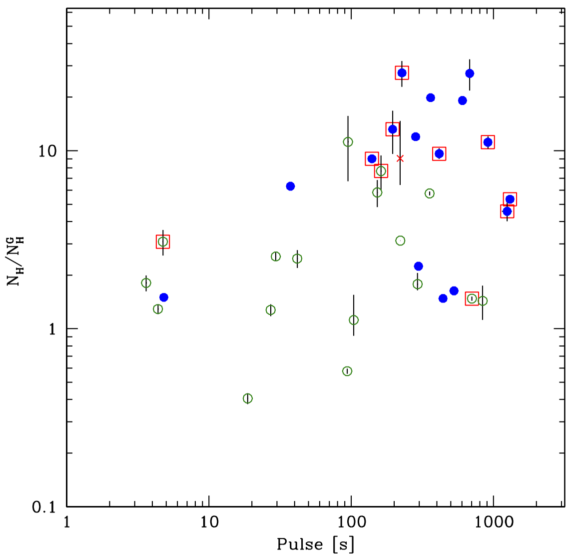

Figure 7. Spin period as a function of reported N_H value (normalized by the expected Galactic value from [5]) for HMXBs detected by ISGRI whose companions are OB supergiants (16, filled circles), Be stars (17, empty circles), or unclassified (1, cross). IGRs are boxed and Magellanic Cloud sources are excluded.

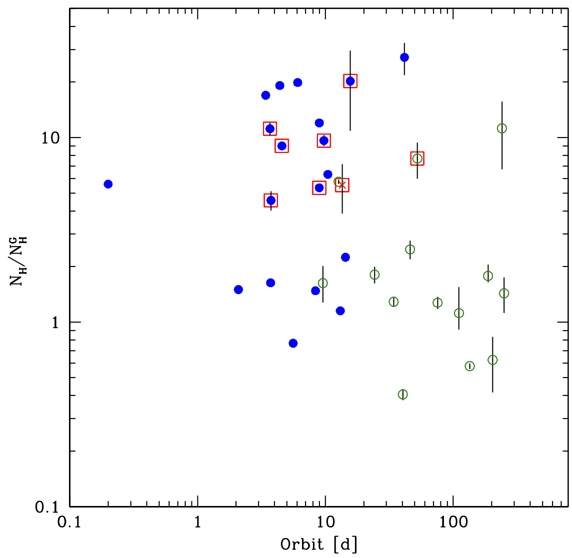

Figure 8. Orbital period versus reported N_H value (normalized by the expected Galactic value from [5]) for HMXBs detected by ISGRI whose companions are OB supergiants (19, filled circles), Be stars (14, empty circles), or unclassified (1, cross). IGRs are boxed and Magellanic Cloud sources are excluded.

tic plane. The main reason that more absorbed sources are being found is that by operating above 20 keV, ISGRI is immune to the absorption that prevented their discovery with earlier soft X-ray telescopes. A large absorption is also a common feature of extragalactic IGRs. However, as a group, they are not more absorbed than pre-*INTEGRAL* AGN [18].

3.3. Modulations

The strong magnetic fields in some NS X-ray binaries can produce hot spots where accretion is favored. If the magnetic and rotation axes are misaligned, this hot spot can result in pulsations in the X-ray light curve. Most IGRs for which a pulsation has been measured have spin periods (P_s) in the range of 100–1000 s, or slightly longer than the average pulse period of pre-*INTEGRAL* sources (Fig. 4). There are notable IGRs that represent extreme cases: IGR J00291+5934 has a pulse period of only 2 ms making it the fastest accretion-powered pulsar ever observed [19], whereas IGR J16358−4726 could have a spin period as long as 6000 s [16].

The distribution of orbital periods (P_o) of IGRs exhibits a similar bimodal shape to that seen in the distribution of orbital periods known before *INTEGRAL* (Fig. 5). The bimodal distribution represents 2 underlying populations: LMXBs (and CVs) which tend to have short orbital periods, and HMXBs which tend to have longer orbital periods.

In a Corbet P_s–P_o diagram [20], members of each subclass of HMXBs segregate into different regions of the plot owing to the complex feedback processes between the modulation periods and the dominant accretion mechanism. Fig. 6 shows that the majority of IGRs are located among other known SG HMXBs. The figure also shows that Be HMXBs have longer orbital periods than SG HMXBs, in general. While this fact was already known [e.g. 21], the discrepancy remains even though *INTEGRAL* has nearly doubled the number of such systems.

3.4. Modulations vs. Absorption

Accretion affects the spin period of a NS. If the velocity at the corotation radius (the radius at which the magnetic field regulates the motion of matter) exceeds the Keplerian velocity, then material will be spun away taking angular momentum with it and the NS will slow down due to the "propellor mechanism" [22]. For corotation velocities smaller than the Keplerian velocity, the material is able to accrete onto the NS magnetosphere which will either spin up or spin down the NS depending on whether the angular momentum of the accreted material has the same or an opposite direction as the NS spin [3]. So the spin rate of the pulsar in a HMXB is regulated by, among other things, the angular momentum of the wind of the stellar companion.

Assuming spherically-symmetric accretion from a radiation-driven wind of a SG star, the density of the wind as a function of radius is $\rho(r) \propto r^{-2}$. On the other hand, the structure of the winds of Be stars is believed to consist of dense slow equatorial outflows and thin fast polar winds [23]. The density drops much faster with the radius ($\rho(r) \propto r^{-3}$) [24]. Therefore, the winds of Be stars present stronger density and velocity gradients inside the capture radius of the NS, in both radial and azimuthal directions, which suggests that wind-fed accretion is more efficient at delivering angular momentum to the NS in Be HMXBs than it is in SG HMXBs [3].

Given the density structures described above, and assuming a steady accretion rate of material whose angular momentum has the same direction as the spin of the NS, the spin period of the NS will reach an equilibrium value $P_{\rm eq} \propto \rho^{-3/7}$. However, the present-day spin periods of NS in SG systems are much longer than predicted and are actually closer to $P_{\rm eq}$ of the stellar winds while the star was still on the MS [3]. The equilibrium spin period in Be systems is constantly adjusting to the changing conditions in the winds [3]. As with the SG systems, pulsars in Be systems are not currently spinning at $P_{\rm eq}$ but reflect the values of an earlier evolutionary stage [25].

With a few exceptions, HMXBs from the Milky Way that have been detected by ISGRI are segregated into distinct regions of a $P_{\rm s}$–$N_{\rm H}$ diagram (Fig. 7) stemming from the higher average $N_{\rm H}$ and longer average $P_{\rm s}$ of SG HMXBs compared to Be HMXBs. The $N_{\rm H}$ values of sources in Fig. 7 have been normalized by the line-of-sight values ($N_{\rm H}^{\rm G}$) from [5]. The SG HMXBs set apart from the others ($P_{\rm s} < 50$ s) are Cen X-3 which is a Roche-lobe overflow system, and OAO 1657−415 which might be transitioning from a wind-fed to a disk-fed system. There could be a weak positive correlation between the $N_{\rm H}$ and spin period for HMXBs as a group. There are no highly-absorbed sources ($N_{\rm H} > 10^{23}$at·cm^{-2}) with spin periods shorter than a few tens of seconds, and there are no pulsars with $P_{\rm s} > 100$ s that are poorly absorbed ($N_{\rm H} < 10^{22}$at·cm^{-2}). A least-squares fit to the data yields $P_{\rm s} \propto N_{\rm H}^{5/8}$. If we consider the $N_{\rm H}$ to be a reliable estimate of the density of matter around the compact object, then the slope that we find contradicts the slope expected from the equilibrium values ($\sim -3/7$). However, the pulsars in Fig. 7 are spinning at longer periods than their equilibrium values would suggest, and the slope that we derive, if real, is subject to heavy uncertainty.

Since Be HMXBs tend to have longer orbital periods than SG HMXBs (see Fig. 6), a distinction is also seen among the distributions of the $N_{\rm H}$ values and orbital periods of HMXBs with Be or SG companions (Fig. 8). There also appears to be a weak anti-correlation of $N_{\rm H}$ and orbital period ($P_{\rm o} \propto N_{\rm H}^{-1/2}$). In both types of systems, a short orbital period implies a compact object that is embedded deeper or spends more time in the dense regions of its stellar companion's wind resulting in more absorption. Therefore, Be HMXBs continue the trend set by SG HMXBs into long-orbital periodicity and low-$N_{\rm H}$ regions of the plot.

Spearman rank tests to the $P_{\rm s}$–$N_{\rm H}$ and $P_{\rm o}$–$N_{\rm H}$ distributions return weak positive and negative correlations with coefficients of 0.33 and −0.33, respectively, suggesting that the null hypothesis of mutual independence between $N_{\rm H}$ and $P_{\rm s}$ or $P_{\rm o}$ can be rejected. From Monte Carlo simulations, we determined that the probability of finding a Spearman rank coefficient $\gtrsim 0.33$ is around 6%. Admittedly, the scatter in the data is large as can be seen in Figs. 7– 8. Because there are large uncertainties in the $N_{\rm H}$ and practically no uncertainty in the spin and orbital periods, the slope from a least-squares fit will tend to overestimate the real slope. Futhermore, the conclusions that we derive for how divergent species of objects react to changes in the local absorbing matter are based on a simplification of the underlying physics. The inclinations of the systems and their eccentricities, for example, are ignored. Even if we can not fit a slope of $-3/7$ to the data in Fig. 7, the slope that we measure could simply be due to the segregation of the 2 populations into different regions of the plots. For example, plotting only the SG HMXBs reduces the significance of the correlations considerably.

Nevertheless, as more sources are added to these diagrams, the potential trends that have emerged could help constrain models describing the influence of local absorbing matter on the modulations. The diagrams might also serve as new tools to help distinguish between SG and Be HMXBs when only $N_{\rm H}$ and either the spin or orbital periods are known. For example, IGR J19140+0951 has an orbital period of around 13 days and $N_{\rm H} \sim 10^{23}$at·cm^{-2}. It is positioned among other SG HMXBs so its companion is probably an OB supergiant (boxed cross in Fig. 8). This designation has already been suggested based on other criteria such as the source's persistent emission. Similarly, AX J1749.2−2725 which is currently an unclassified HMXB could have a SG companion based on its position in Fig. 7 ($N_{\rm H} > 10^{23}$at·cm^{-2} and pulse period over 100 s).

4. SUMMARY & CONCLUSIONS

Of the 343 sources that ISGRI has detected, 70 are HMXBs, 76 are LMXBs, 39 are miscellaneous Galactic sources, 88 are AGN, and 70 remain unclassified. Clustered towards the spiral arm tangents and at low Galactic latitudes, HMXBs follow the distributions of tracers of star-forming regions. In contrast, most LMXBs huddle in the Galactic bulge or have had time to migrate to high latitudes, typical of an older stellar population. The discrepancy is seen again in galactocentric profiles where the number of LMXBs gradually decreases from its maximum in the central kpcs, while HMXBs avoid the central kpcs and are overrepresented at the peaks of HII/CO distributions. Over 140 new sources have been discovered by ISGRI but many of them remain unclassified. The spatial distribution of unclassified sources resembles a Galactic population rather than an extragalactic one, although some are AGN behind the plane.

Since it operates above 20 keV and is unhindered by absorption, ISGRI is discovering many new HMXBs (30) and AGN (39) that are heavily-absorbed ($N_{\rm H} \sim 10^{23}$ at·cm^{-2}). On average, Galactic IGRs are more absorbed (by a factor of ~4) than sources that were previously known. Fourteen new CVs have been found but only 3 new LMXBs since their typically lower column densities means they were likely already known before *INTEGRAL*.

Spin periods for most IGR pulsars are between a few hundred to a few thousand seconds or somewhat longer than the average spin periods of sources known before *INTEGRAL*. The distribution of orbital periods for IGRs closely resembles the bimodal distribution set by previously-known sources. The peaks represent 2 underlying populations: LMXBs and CVs with short orbital periods, and HMXBs with long orbital periods. Almost all IGRs for which both spin and orbital periods have been measured are located in the region of wind-fed accretion in the Corbet diagram. This is a testament to the number of new SG HMXBs that *INTEGRAL* has discovered.

Two new plots have been created to test for dependences of the spin and orbital periods of HMXBs on the amount of absorbing matter local to the source. While scatter is an issue, there is a clear segregation of HMXBs in both plots which could be used to help assign Be or SG companions to sources that are still unclassified. There could be trends in both the P_s–N_H and P_o–N_H diagrams. The possible correlation of $P_s \propto N_H^{5/8}$ appears to contradict the expected slope $(-3/7)$ which could be further proof that current spin periods are longer than the predicted equilibrium values, and that the spin-up of the pulsar via the wind is not as effective as the spin-down via the "propellor mechanism." The potential anti-correlation in the P_o–N_H plot means that the average column density varies inversely with the distance between the objects as one would expect.

This work takes advantage of multi-wavelength observations in order to understand the nature of IGRs, and to help clarify the mechanisms that govern each type of source. Among the challenges facing more detailed population studies is the limited sample size of each subclass. This can only be alleviated by using large-FOV instruments such as *INTEGRAL* to search for new sources, and by regularly observing each new source in other wavelengths so that the accumulation of evidence rules out all but a single type of object. Many of the new sources which have been classified are absorbed HMXBs with supergiant companions. The increasing number of these systems discovered by *INTEGRAL* could alter our view of the Galactic population of hard X-ray sources and the evolutionary scenarios of their massive stellar companions.

ACKNOWLEDGMENTS

AB warmly thanks the Moscow LOC, C. Winkler, and the referee. AB acknowledges D.R. Willis, S.E. Shaw, G. Wendt, S. Paltani and M. Tuerler. This publication uses observations obtained with the ESA science mission *INTEGRAL*.The *INTEGRAL* instrument and data centres were directly funded by ESA member states and the USA (NASA). This research used NASA's Astrophysics Data System Bibliographic Services and the SIMBAD database, operated at CDS, Strasbourg, France.

REFERENCES

[1] Lebrun F., Leray J. P., Lavocat P., et al., 2003, A&A, 411, L141

[2] Ubertini P., Lebrun F., Di Cocco G., et al., 2003, A&A, 411, L131

[3] Waters L. B. F. M. & van Kerkwijk M. H., 1989, A&A, 223, 196

[4] Courvoisier T. J.-L., Walter R., Rodriguez J., et al., 2003, IAU Circ., 8063, 3

[5] Dickey J. M. & Lockman F. J., 1990, ARA&A, 28, 215

[6] Walter R., Courvoisier T. J.-L., Foschini L., et al., 2004, in *The INTEGRAL Universe. Proceedings of the Fifth INTEGRAL Workshop*, ESA SP-552, 417

[7] Kuulkers E., 2005, in AIP Conf. Proc. 797: *Interacting Binaries: Accretion, Evolution, and Outcomes*, 402

[8] Rodriguez J., Bodaghee A., Kaaret P., et al., 2006, MNRAS, 366, 274

[9] Bodaghee A., Walter R., Zurita Heras J. A., et al., 2006, A&A, 447, 1027

[10] Zurita Heras J. A., de Cesare G., Walter R., et al., 2006, A&A, 448, 261

[11] Sguera V., Barlow E. J., Bird A. J., et al., 2005, A&A, 444, 221

[12] Ebisawa K., Bourban G., Bodaghee A., et al., 2003, A&A, 411, L59

[13] Stephen J. B., Bassani L., Malizia A., et al., 2006, A&A, 445, 869

[14] Vallée J. P., 2002, ApJ, 566, 261

[15] Masetti N., Morelli L., Palazzi E., et al., 2006, A&A, 459, 21

[16] Lutovinov A., Revnivtsev M., Gilfanov M., et al., 2005, A&A, 444, 821

[17] Dean A. J., Bazzano A., Hill A. B., et al., 2005, A&A, 443, 485

[18] Beckmann V., Soldi S., Shrader C. R., et al., 2006, ApJ, 652, 126

[19] Galloway D. K., Markwardt C. B., Morgan E. H., et al., 2005, ApJL, 622, 45

[20] Corbet R. H. D., 1984, A&A, 141, 91

[21] Stella L., White N. E., & Rosner R., 1986, ApJ, 308, 669

[22] Illarionov A. F. & Sunyaev R. A., 1975, A&A, 39, 185

[23] Lamers H. J. G. L. M. & Waters L. B. F. M., 1987, A&A, 182, 80

[24] Waters L. B. F. M., van den Heuvel E. P. J., Taylor A. R., et al., 1988, A&A, 198, 200

[25] King A. R., 1991, MNRAS, 250, 3

[26] Corbet R. H. D., 1986, MNRAS, 220, 1047